Interfacial Active Fluorine Sites Induced Electron Transfer on TiO$_2$ (001) Facets to Enhance Polysulfide Redox Reactions for Better Liquid Li$_2$S$_6$-Based Lithium Sulfur Batteries

Chenyang Zha,[a, *, ‡] Xiuquan Gu,[b, ‡] Donghai Wu,[c, ‡] Houyang Chen[d, *]

[a] Key Laboratory of Flexible Electronics (KLOFE), Institute of Advanced Materials (IAM), Jiangsu National Synergistic Innovation Center for Advanced Materials (SICAM), Nanjing Tech University, Nanjing Jiangsu 211816, China

[b] School of Materials Science and Engineering, China University of Mining and Technology, Xuzhou 221116, China

[c] Henan Provincial Key Laboratory of Nanocomposites and Applications, Institute of Nanostructured Functional Materials, Huanghe Science and Technology College, Zhengzhou 450006, China

[d] Department of Chemical and Biological Engineering, State University of New York at Buffalo, Buffalo, New York 14260-4200, USA

‡ These authors contributed equally to this work.

* Corresponding authors:
E-mail: zha@suda.edu.cn
E-mail: hchen23@buffalo.edu

Contents

S1. Experimental Section

The fluorine doped TiO_2 nanosheets (F-TiO_2) were synthesized through a facile hydrothermal reaction. In a typical synthesis, 12-16 mL of acetic acid and 5-8 mL of deionized water were added to a plastic baker, and then 0.2-0.4 g ammonium fluoride was added to the above solution and stirred for 20 min (ammonium fluoride is extremely corrosive and toxic. It should be handled with extreme care). Subsequently, 0.4-0.6 ml tetrabutyl titanate was added to the solution under stirring to form a clear solution. The reaction solution was transferred into a 60 mL Teflon-lined autoclave and heated at 160 ^{o}C for 10 h. After being cooled to room temperature, the precipitate was collected and washed repeatedly with deionized water and ethanol, then dried at 60 ^{o}C for 12 h. Next, the as-prepared samples were annealed in the oxygen atmosphere at 500 ^{o}C for 2 h. Final, F-TiO_2 samples were successfully synthesized.

S2. Material Characterization

The structures of the samples were characterized using Powder X-ray diffraction (XRD) analysis (PANalytical, Empyrean). The morphologies and microstructures of the samples were characterized by both optical microscopy and field emission scanning electron microscopy (SEM, Zeiss Super 55 instrument operated at 5-15 kV). Transmission electron microscopy (TEM) images were acquired using a JEM 2100F transmission electron microscope at an acceleration voltage of 200 kV. In-situ X-ray photoelectron spectroscopy (XPS) measurements were carried out on a Thermo Scientific Nexsa XPS system with a monochromatic Al Kα radiation (hv = 1486.7 eV) and a concentric hemispherical analyzer. Before all in-situ XPS measurements, the batteries were disassembled inside an argon-filled glovebox, and the sample electrodes were carefully rinsed with 3 ml mixed solvents of 1,3-dioxolane (DOL) and 1,2-dimethoxyethane (DME) with a volume ratio of 1:1. The samples were transferred with a specially-built airtight bottle from the glovebox to the spectrometer, to reduce air exposure during the entire sample preparation and transfer processes. The XPS data analysis was carried out using Avantage software.

S3. Electrochemical Characterization

The electrochemical measurements were implemented using the CR2032-type coin cell. The cells were assembled in an argon-filled glove box (H_2O and O_2< 0.2 ppm). The electrode film was prepared by mixing 70 wt% of F-TiO_2 material, 20 wt%

of conductive carbon and 10 wt% of polyvinylidene fluoride in N-methylpyrrolidone, then the slurry was casted on the carbon cloth and dried at 120 °C for 24 h. A high pure lithium foil and Celgard 2400 membrane were used as the counter electrode and the separator, respectively. The electrodes were protected by carbon paper. For one electrode (area: 2 cm^2), the active sulfur mass loading was about 1.0-3.0 mg/cm^2.

The high purity electrolyte was composed of 1 M bis(trifluoromethane) sulfonamide lithium salt (LiTFSI) and 0.5 M LiNO$_3$ dissolved in mixed solvents of 1,3-dioxolane (DOL) and 1,2-dimethoxyethane (DME) with a volume ratio of 1:1. Then, Li$_2$S and sulfur powder (molar ratio of 1 : 5) were added into the high purity electrolyte to form 0.5 M Li$_2$S$_6$ (Li$_2$S + 5S = Li$_2$S$_6$, molar concentration calculated based on S atom). 20-25 μl/cm^2 electrolytes and 20-40 % (mass fraction) F-TiO$_2$ are provided in per cell. The mixture was heat-treated on the hot plate at 50 °C with continuous stirring in the Ar atmosphere to form a uniform catholyte solution. The cathode was then impregnated with a calculated amount of the Li$_2$S$_6$-containing catholyte. The galvanostatic discharge-charge experiments were performed over a voltage range of 1.8-2.6 V (vs. Li/Li$^+$) at different rates using a NEWARE BTS and LAND (CT2001A) battery tester. The capacities and C-rate currents were based on active materials-sulfur (1 C corresponding to 1600 mA·g^{-1}). Electrochemical impedance spectroscopy (EIS) measurements were carried out on a Gamry potentiostat by applying a sine wave with the amplitude of 10 mV over the frequency range from 100 kHz to 1 mHz. Cyclic voltammetry (CV) was performed using the CHI660E potentiostat at a scanning rate of 0.1 mV·s^{-1}. All cells were aged and then activated for several cycles before the cyclic test.

S4. Theoretical Calculations

The first-principles calculations were carried out using the Vienna *ab initio* Simulation Package (VASP) with the projector augmented wave method (PAW).[1-3] The exchange-correlation potential is described by the generalized gradient approximation of Perdew-Burke-Ernzerhof (GGA-PBE)[1-3] with a cut off energy of 500 eV for the expansion of the electronic wave function in the plane waves basis set. All the atomic positions and geometries are full relaxed until the total energy and Hellmann-Feynman forces are less than 10^{-5} eV and 0.01 eV/Å, respectively. The Brillouin-zone

integrations are performed with a Gaussian smearing of 0.05 eV over a 3 x 3 x 1 Monkhorst-Pack k-point mesh. A six layers p(3 x 3) slab model was used to describe the anatase TiO_2 (001) surface (Fig. S6a), where the upper half of the Ti and O atoms in the super cell were relaxed. The lower half was fixed initially as those in the bulk with optimized lattice parameters of 3.81 Å and 9.61 Å (which are compared to the experimental results of 3.87 Å and 9.62 Å.[1-5] Each of these Ti_{5c} atoms is bonded to two raised O_{2c} and two lowered O_{3c} atoms in the [100] and [010] directions, respectively (Fig. S6a). The supercell consists of 54 TiO_2 units (162 atoms in total), and periodically repeated slabs are separated by a vacuum space of 15 Å.

References

1.   J. P. Perdew, K. Burke and M. Ernzerhof, *Phys. Rev. Lett.*, 1996, **77**, 3865.
2.   G. Kresse and J. Furthmuller, *Phys. Rev. B*, 1996, **54**, 11169-11186.
3.   P. E. Blöchl, *Phys. Rev. B*, 1994, **50**, 17953.
4.   U. Diebold, *Surf. Sci. Rep.*, 2003, **48**, 53-229.
5.   Q. Lin, Q. Li, C. BatchelorMcAuley and R. G. Compton, *Phys. Chem. Chem. Phys.*, 2013, **15**, 7760-7767.

Table S1. Electrochemical performance of the F-TiO$_2$-based Li$_2$S$_6$ cell and other similar cathode materials reported in literature.

| Polysulfide hosts	S loading [mg/cm^2]	Current density [mA/cm^2]	Cycling stability [mAh/g]	Reference
F-TiO$_2$	1.0	0.8	1030 after 500 cycles	**This work**
	2.0	1.6	712 after 500 cycles	
	3.0	1.6	480 after 500 cycles	
	3.0	3.2	500 after 500 cycles	
3DTiO$_2$	1.5-2.0	0.5-0.6	797 after 240 cycles	*Small* **2017**, 13, 1701013
	1.5-2.0	2.5-3.3	608 after 700 cycles	
TiO	1.5	0.67	750 after 500 cycles	*Nat. Commun.* **2016**, 7, 13065.
	4.0	0.33	821 after 500 cycles	
MoS$_{2-X}$	1.5	1.6	816 after 600 cycles	*Energy Environ. Sci.* **2017**, 10, 1470.
VN	3.0	3.2	907 after 200 cycles	*Nat. Commun.* **2017**, 8, 14627.
TiO$_2$-TiN	1.2	3.2	551after 2000 cycles	*Energy Environ. Sci.* 2017, 10, 1694.
	3.1	3.2	350 after 2000 cycles	
	4.3	3.2	328 after 2000 cycles	
W$_2$C	1.0	0.64	1044 after 200 cycles	*Nano Lett.* **2018**, 18, 1035.
Mo$_2$C	1.0	0.64	972 after 200 cycles	
TiC	1.0	0.64	858 after 200 cycles	
Phosphorene	3.3	3.2	663 after 500 cycles	*Adv. Mater.* **2017**, 29, 1602734.
Carbon nanotube sheet	10	1.6	615 after 500 cycles	*Adv. Sci.* **2018**, 5, 1800384.
N,S-codoped graphene	8.5	1.6	666 after 200 cycles	*Nat. Commun.* **2015,** 6, 7760.
3DNG/TiN	4.8	3.2	888 after 200 cycles	*Adv. Mater.* **2018**, 30, 1804089
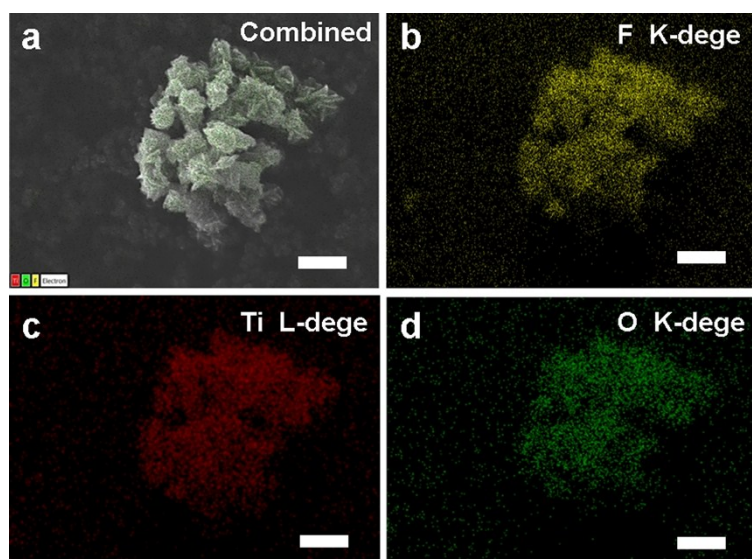
Fig. S1 SEM image (a) and elemental mapping images of F-TiO$_2$ with fluorine (b), titanium (c) and oxygen (d) elements. The bar scale is 2 μm.
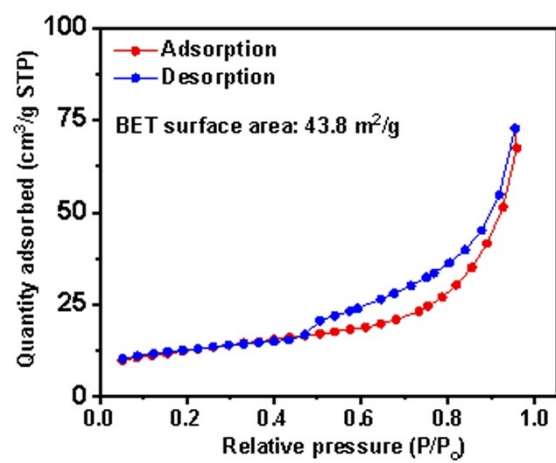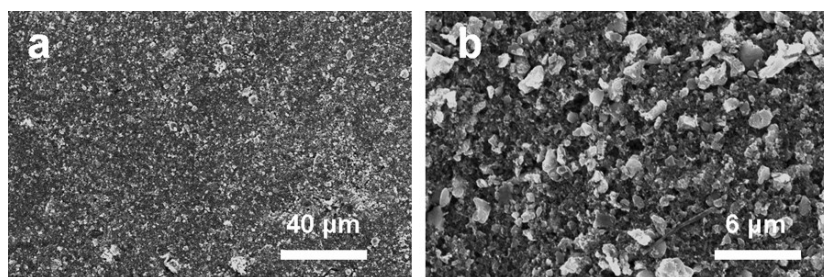
Fig. S2 Adsorption-desorption isotherms of N_2 on F-TiO$_2$.
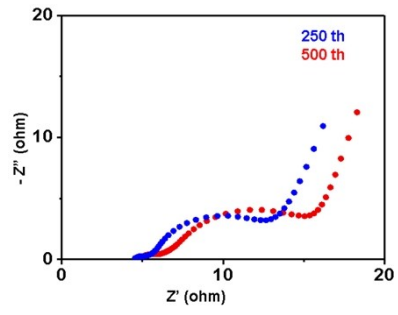
Fig. S3 SEM of the F-TiO$_2$ electrode.

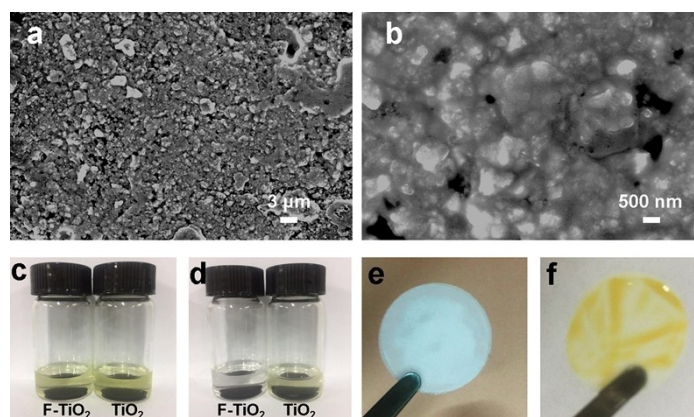**Fig. S4** The magnified Nyquist plots (0-20 ohm) of cells.

Fig. S5 SEM images of Li_2S_6-F-TiO_2 electrodes after a cell running (a-b). The optical photos of F-TiO_2 and TiO_2 materials soaked in the Li_2S_6 solution at beginning (c) and after 2 h (d). The optical photos of the separator before (e) and after (f) the Li-S cell cycling.
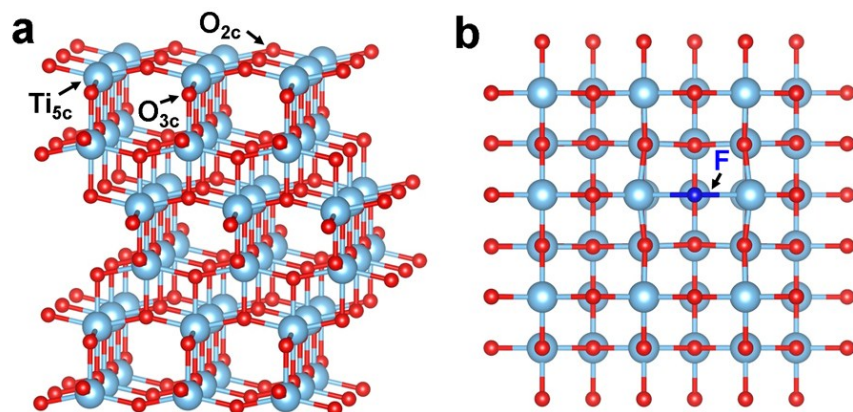
Fig. S6 (a) The periodic slab model used for TiO_2 (001) facets. (b) Top view of the most stable configuration of $F-TiO_2$ (001) facets.
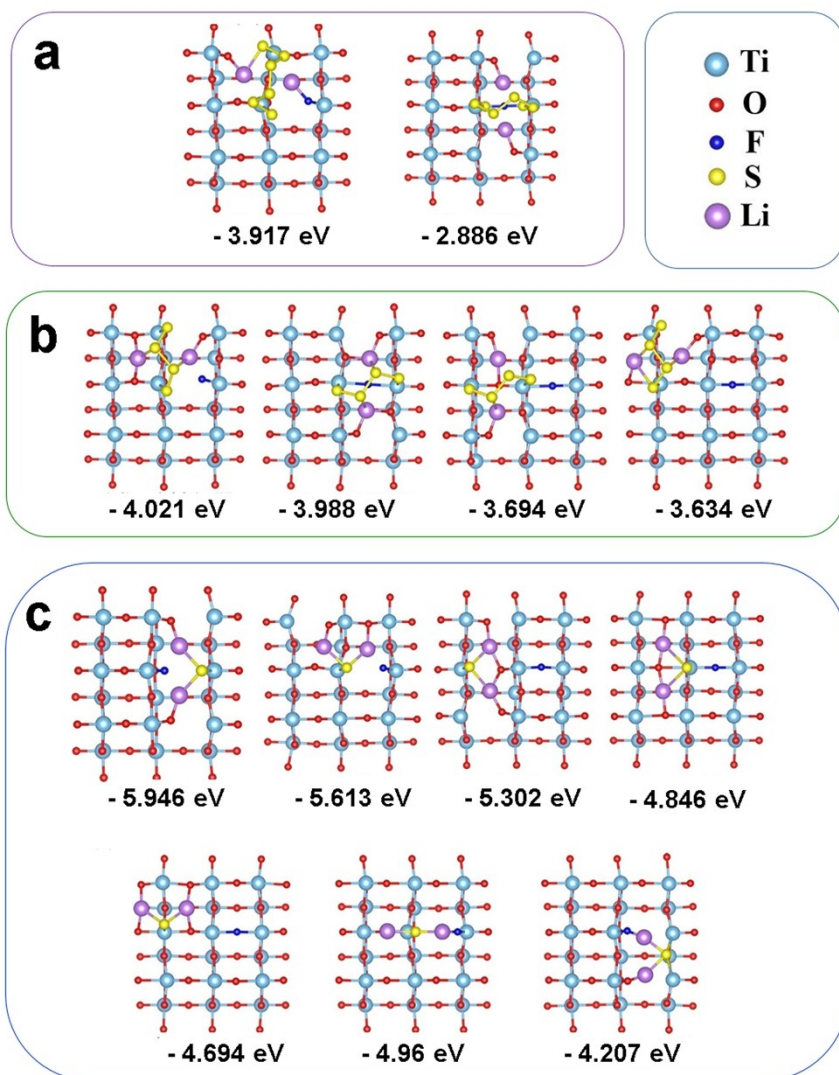
Fig. S7 Top views of the possible adsorption configurations of Li_2S_6 (a), Li_2S_4 (b) and Li_2S (c) on F-TiO_2 (001) facets. The corresponding adsorption energies are listed in bottom.